Cherenkov radiation and scattering of external dispersive waves by two-color solitons

Ivan Oreshnikov,[1,*] Oliver Melchert,[2,3,4] Stephanie Willms,[2,3] Surajit Bose,[2,5] Ihar Babushkin,[2,3] Ayhan Demircan,[2,3,4] Uwe Morgner,[2,3,4] and Alexey Yulin[6]

[1]*Max Planck Institute for Intelligent Systems, Max-Planck-Ring 4, 72076 Tübingen, Germany*
[2]*Cluster of Excellence PhoenixD, Welfengarten 1, 30167 Hannover, Germany*
[3]*Leibniz Universität Hannover, Institute of Quantum Optics, Welfengarten 1, 30167 Hannover, Germany*
[4]*Hannover Centre for Optical Technologies, Nienburger Strasse 17, 30167 Hannover, Germany*
[5]*Leibniz Universität Hannover, Institute of Photonics, Nienburger Strasse 17, 30167 Hannover, Germany*
[6]*Department of Physics, ITMO University, Kronverskiy Prospekt 49, 19701 St. Petersburg, Russia*

(Received 12 July 2022; accepted 11 October 2022; published 22 November 2022)

For waveguides with two separate regions of anomalous dispersion, it is possible to create a quasistable two-color solitary wave. In this paper, we consider how those waves interact with dispersive radiation, i.e., both the generation of Cherenkov radiation and the scattering of incident dispersive waves. We derive the analytic resonance conditions and verify them through numeric experiments. We also report incident radiation driving the internal oscillations of the soliton during the scattering process in the case of an intense incident radiation. We generalize the resonance conditions for the case of an oscillating soliton and demonstrate how one can use the scattering process to probe and excite an internal mode of two-color soliton molecules.

DOI: 10.1103/PhysRevA.106.053514

I. INTRODUCTION

Solitary waves or solitons are localized nonlinear excitations that preserve their shapes during evolution. In the systems close to integrable ones, solitons are proven to be robust and, in many cases, different interactions result only in the variation of the soliton parameters, such as its intensity or frequency. In a certain sense, solitons can be called "eigenmodes of the nonlinear problem," meaning that the dynamics of the system can be considered as a set of solitons interacting with quasilinear dispersive waves. Due to their robustness, solitons are of fundamental as well as practical importance, for example, in the context of optical supercontinuum generation [1–3] or soliton fiber lasers [4–7].

The mutual interaction of optical solitons in fibers can enable the formation of bound states, often referred to as soliton molecules. They can be realized via dispersion engineering in the framework of the standard nonlinear Schrödinger equation (NLS) and consist of two pulses that maintain a fixed separation in time [8,9]. Further, optical soliton clusters have been discovered and studied in a large variety of physical systems described by different equations, such as the generalized nonlinear Schrödinger equation [10–12], coupled NLSs [13,14], the Ginzburg-Landau equation [15,16], Lugiato-Lefever equation [17], and many others [18–28]. The aforementioned bound states of solitons have a single central frequency and the whole spectrum is localized around this frequency.

Another possibility to observe soliton molecules is to provide interaction between solitons having their carrier frequencies well detuned from each other. To make the interaction efficient, the velocities of the solitons must be close. In the case of scalar solitons, this means that we need higher-order dispersion with two different frequency ranges where the solitons can be accommodated. These solitons were recently reported in [29–32] for pulses propagating in conservative fibers with higher-order dispersion. Similar solitons were also discovered in mode-locked cavity lasers [33] and in coherently pumped ring resonators [34,35].

In the case of nonintegrable systems, solitons can interact with dispersive waves (DWs) of low intensity and this interaction leads to interesting physical phenomena, such as the efficient generation of new frequencies [36–40]. It should be noted that this effect is closely related to the optical push-broom effect [41]. Such resonant scattering can be cascaded, enriching optical supercontinuum spectra significantly [42]. Similar effects were studied in Refs. [43–45], where the term "optical event horizon" was coined. It was also established that resonant dispersive waves affect the parameters of the solitons and can lead to dispersive wave mediated acceleration of solitons [37,43,46–50]. It should be mentioned that the resonant scattering of dispersive waves is also studied for dark solitons [51–54] and oscillating solitons [55–60].

The present paper aims to study in detail the interaction of dispersive waves with two-color soliton molecules, consisting of two bound solitons having well-separated frequencies. In the prior work [29], we have demonstrated how to create quasistable configurations of two tightly coupled pulses in a dispersion landscape $\beta(\omega)$ with two regions of anomalous dispersion, separated by a region of normal dispersion. Each of these subpulses propagates on its own carrier frequency. This coupled state, especially in the process of initial evolution, sheds dispersive waves that resemble Cherenkov radiation that

*oreshnikov.ivan@gmail.com

is observed for other types of solitary waves in a vast variety of settings [56–58,60–62]. Let us remark that there is a well-established tradition in the community to draw the analogy between the resonant radiation of solitons and Cherenkov radiation of charged particles. However, the Cherenkov effect is just one example of the very general phenomenon of the emission of the phase-matched wave by a moving object.

Since DW generation is demonstrated, it is reasonable to anticipate that two-color soliton molecules colliding with DWs will produce resonant emission in the same way as it occurs in the case of conventional solitons. Thanks to a more complex structure of the two-color solitons, one can expect the scattering dynamics to be much richer compared to the conventional single soliton case. For instance, it is possible that the internal degrees of freedom can be excited due to the interaction with a DW and this should strongly affect the dynamics of the system. Subsequently, we confirm this influence, providing a combined analytical and numerical view of the process.

The paper is structured as follows. In Sec. II, we introduce a mathematical model for the light propagating in a nonlinear fiber with higher-order dispersion and derive the condition of resonant four-wave mixing of the soliton molecules with DWs. In Sec. III, we report the results of the numerical simulations of the different propagation regimes of bichromatic soliton molecules. The results of the simulations are compared against analytical resonance conditions. Section IV discusses the weakly nonlinear case where the intensity of the dispersive waves is sufficiently large to modify the interaction between the soliton molecules and the waves. The excitation of the internal mode is also discussed in this section. The paper concludes with a summary in Sec. V.

II. ANALYTICAL MODEL

In this section, we derive a perturbation theory that explains the resonance conditions that were proposed in [29], demonstrate additional Cherenkov radiation mechanisms due to four-wave mixing (FWM) between the frequency components of the soliton, and then extend this theory to describe the process of scattering of external waves on the soliton.

We start by considering a nonenvelope version of a nonlinear Schrödinger equation [63],

$$i\partial_z\tilde{u} + \beta(\omega)\tilde{u} + \gamma(\omega)\mathcal{F}\{|u|^2u\}_{(\omega>0)} = 0. \tag{1}$$

Here and further, $\tilde{u} \equiv \tilde{u}(z,\omega)$ indicates the Fourier image of the field $u \equiv u(z,t)$, and $\mathcal{F}\{\cdots\}_{(\omega>0)}$ is the explicit Fourier transform taken for the positive frequencies only.

To build the perturbation theory, let us introduce an ansatz that represents the solution as a sum of two single-frequency solitary waves $U_{1,2}(z,t)$ and a small residue radiation $\psi(z,t)$,

$$u(z,t) = U_1(z,t) + U_2(z,t) + \psi(z,t), \quad |\psi| \ll |U_1| \sim |U_2|. \tag{2}$$

For the solitary waves $U_{1,2}(z,t)$, we assume that they satisfy a pair of coupled nonlinear Schrödinger equations below,

$$i\partial_z U_n + \beta_n(i\partial_t)U_n(z,t) + \gamma(\omega_n)\big(|U_n|^2U_n + 2|U_m|^2U_n\big) = 0, \tag{3}$$

where $n = 1, 2$ and $m = 2, 1 \neq n$. Essentially, this is an assumption that the two-color soliton molecule consists of two pulses, which are incoherently coupled by inducing a refractive-index potential on each other [64]. Each subpulse exists in some sort of truncated dispersion landscape, defined by the operator $\beta_n(i\partial_t)$. Under specific conditions, the subpulses are given by fundamental solitons of a modified NLS [31]. A reasonable guess for the truncated operator is a parabolic approximation close to the carrier frequency,

$$\beta_n(i\partial_t) = \beta(\omega_n) + i\beta'(\omega_n)\partial_t - \tfrac{1}{2}\beta''(\omega_n)\partial_t^2. \tag{4}$$

Let us remark that this simple approximation of the dispersion is absolutely relevant physically. We acknowledge that the high-order terms can modify the shape of the soliton but, apart from the special cases that require separate consideration, the influence of these terms is only quantitative.

We additionally suppose that in the soliton's frame of reference, the envelope evolves with wave number $k_n(\omega)$, which we approximate by the wave number of the fundamental soliton in the ordinary nonlinear Schrödinger equation and a correction from a secondary soliton as

$$k_n(\omega) \approx \frac{\gamma(\omega_n)A_n^2}{2} + \beta(\omega_n) + \beta'(\omega_n)(\omega-\omega_n) + \gamma(\omega_n)A_m^2, \tag{5}$$

where $n = 1, 2, m = 2, 1 \neq n$, and A_n is the soliton amplitude.

By substituting ansatz (2) into Eq. (1), linearizing with respect to perturbation $\psi(z,\omega)$, and discarding the terms corresponding to the soliton given by Eqs. (3), we get the equation for $\tilde{\psi}$,

$$\begin{aligned} i\partial_z\tilde{\psi} + \beta(\omega)\tilde{\psi} + \gamma(\omega)\mathcal{F}\big\{&2|U_1 \\ &+ U_2|^2\psi + (U_1+U_2)^2\psi^*\big\}_{(\omega>0)} \\ = &-[\beta(\omega)-\beta_1(\omega)]\tilde{U}_1 - [\beta(\omega)-\beta_2(\omega)]\tilde{U}_2 \\ &- \gamma(\omega)\mathcal{F}\big\{U_2^2U_1^* + U_1^2U_2^*\big\}_{(\omega>0)}. \end{aligned} \tag{6}$$

On the right-hand side (rhs) of Eq. (6), we see two types of driving terms and each of those terms can be in resonance with the linear DWs that exist in the system if the particular wave number $k(\omega_*)$ of the driving term is equal to the wave number of a DW $\beta(\omega_*)$ at some frequency ω_* [36,61]. The first type is given by $[\beta(\omega)-\beta_n(\omega)]\tilde{U}_n(z,\omega)$, which drives the generation of Cherenkov radiation by an individual soliton U_n if the following resonance condition is satisfied:

$$\beta(\omega) = k_n(\omega), \tag{7}$$

where the soliton wave vector is given by (5). The second type of terms is $\gamma(\omega)\mathcal{F}\{U_2^2U_1^*\}$ and $\gamma(\omega)\mathcal{F}\{U_1^2U_2^*\}$, which correspond to the process of four-wave mixing that in our case results in the generation of dispersive radiation at some frequency where

$$\beta(\omega) = 2k_n(\omega) - k_m(\omega). \tag{8}$$

Let us move on to the problem of external dispersive wave scattering. For that, we split the perturbation into the incident and the scattered parts,

$$\psi(z,t) = \psi_{\text{inc}}(z,t) + \psi_{\text{sc}}(z,t). \tag{9}$$

We explicitly define $\psi_{\rm inc}(z,t)$ as a linear wave that is propagating in a soliton-free medium,

$$i\partial_z\tilde{\psi}_{\rm inc}(z,t)+\beta(\omega)\tilde{\psi}_{\rm inc}(z,t)=0. \tag{10}$$

Substituting Eq. (9) into (6) and eliminating the terms corresponding to Eq. (10), we are left with the equation for the scattered component,

$$\begin{aligned} &i\partial_z\tilde{\psi}_{\rm sc}+\beta(\omega)\tilde{\psi}_{\rm sc}+\gamma(\omega)\mathcal{F}\left\{2|U_1+U_2|^2\psi_{\rm sc}+(U_1+U_2)^2\psi^*_{\rm sc}\right\}_{(\omega>0)}\\ &\quad=\ldots\ \text{[omitted is the rhs of Eq. (6)]}-\gamma(\omega)\mathcal{F}\left\{2(|U_1|^2+U_1U_2^*+U_2U_1^*+|U_2|^2)\psi_{\rm inc}+\left(U_1^2+2\,U_1U_2+U_2^2\right)\psi^*_{\rm inc}\right\}_{(\omega>0)}. \end{aligned} \tag{11}$$

In addition to the resonance terms already discussed in Eq. (6), we see terms that arise due to the interaction between the incident radiation and the soliton. Here, six new types of resonance behavior are possible. The first one is due to terms $|U_1|^2\psi_{\rm inc}$ and $|U_2|^2\psi_{\rm inc}$, both with the resonance condition

$$\beta(\omega_{\rm sc})=\beta(\omega_{\rm inc}). \tag{12}$$

The next two are due to mixed terms $U_1U_2^*\psi_{\rm inc}$ and $U_2U_1^*\psi_{\rm inc}$, with the corresponding resonance condition being

$$\beta(\omega_{\rm sc})=\pm k_1\mp k_2+\beta(\omega_{\rm inc}). \tag{13}$$

Another two are due to $U_n^2\psi^*_{\rm inc}$ and the resonance condition is

$$\beta(\omega_{\rm sc})=2k_n(\omega_{\rm sc})-\beta(\omega_{\rm inc}),\quad n=1,2. \tag{14}$$

The final one is due to $2U_1U_2\psi^*_{\rm inc}$, with the resonances at

$$\beta(\omega_{\rm sc})=k_1(\omega_{\rm sc})+k_2(\omega_{\rm sc})-\beta(\omega_{\rm inc}). \tag{15}$$

To verify the predictions given by resonance conditions (7), (8), and (12)–(15), we proceed to numerical experiments.

III. NUMERICAL EXPERIMENTS

To numerically integrate Eq. (1), we use the integrating factor method and transform the equation into a nonstiff version for a modified spectrum [3]. The modified equation can be handled by any standard Ordinary Differential Equation (ODE) solver; we use a SCIPY interface to ZVODE solver from ODEPACK [65,66] (the code necessary to reproduce the results in the paper can be found in [67]). All the computations are performed in a frame of reference co-moving with the soliton, which is achieved by a transformation

$$t\to t-\beta'(\omega_1)z,$$

which, in turn, results in

$$\begin{aligned} \beta(\omega)&\to\beta(\omega)-\beta(\omega_1)-\beta'(\omega_1)(\omega-\omega_1),\\ k_1(\omega)&\to\frac{\gamma(\omega_1)A_1^2}{2}+\gamma(\omega_1)A_2^2,\\ k_2(\omega)&\to\frac{\gamma(\omega_2)A_2^2}{2}+\gamma(\omega_1)A_1^2+\beta(\omega_2)-\beta(\omega_1). \end{aligned}$$

A description of the specific dispersion profile model $\beta(\omega)$ used in the simulations can be found in Appendix A.

To study Cherenkov radiation of two-color solitons, we chain two separate simulations. First, following the prior work [29], we produce a two-color soliton by integrating an initial condition that is given by a sum of two fundamental solitons of the standard NLS,

$$u_0(t)=A_1\mathrm{sech}(t/T_1)e^{-i\omega_1 t}+A_2\mathrm{sech}(t/T_2)e^{-i\omega_2 t}, \tag{16}$$

where frequencies ω_1 and ω_2 are both lying in the regions of anomalous dispersion. Frequency ω_1 is otherwise arbitrary; ω_2 is chosen so that the group velocities of both the frequency components match,

$$\beta'(\omega_1)=\beta'(\omega_2).$$

In most of the simulations presented subsequently, we fix $T_1=T_2=20\,$fs and the amplitudes A_1 and A_2 are chosen as the fundamental soliton amplitudes at the corresponding frequencies. This configuration sheds a significant amount of radiation and relaxes to a quasistable solitary wave. We propagate up to $z=10$ cm, take the output field of this seed simulation, and suppress the radiation tails by multiplying it by a super-Gaussian temporal window, centered on the peak of the soliton molecule. This isolated soliton molecule serves as an input to the second simulation that is carried with the same parameters as the original one.

Once we suppress the radiation that is shed by the seed solitons during the initial relaxation process, the isolated two-color soliton molecule propagates generating only a narrow-spectrum Cherenkov radiation. An example is shown in Fig. 1. Figure 1(b) shows the normalized spectral densities at the input and output, i.e., $z=0$ cm and 10 cm, respectively. For clarity, the difference between both spectra is shown on a logarithmic scale in Fig. 1(c). It is clearly evident that on top of the input spectrum [thin black line in Fig. 1(b)], two additional spectral lines appear in the output spectrum [gray line in Fig. 1(b)]. To clarify the origin of these pronounced spectral lines, Fig. 2(d) demonstrates resonance conditions (7) and (8): the black curve corresponds to $\beta(\omega)$, i.e., the left-hand side of both equations; the horizontal lines correspond to the right-hand sides. Intersections between the dispersive curve and the horizontal lines that contribute to Cherenkov radiation are marked separately: ① labels radiation due to the second component of the soliton, as predicted by Eq. (7); ② labels the location of frequencies due to FWM between the frequency components, resulting in radiation with wave number $2k_2-k_1$, as predicted by Eq. (8).

To study the scattering processes, we perform the seed simulation and isolate the two-color soliton. To accomplish that, we add an incident DW in the form of a Gaussian pulse,

$$\psi_{\rm inc}(t)=A_{\rm inc}\exp\left[-\frac{(t-t_0)^2}{T_{\rm inc}^2}-i\omega_{\rm inc}t\right].$$

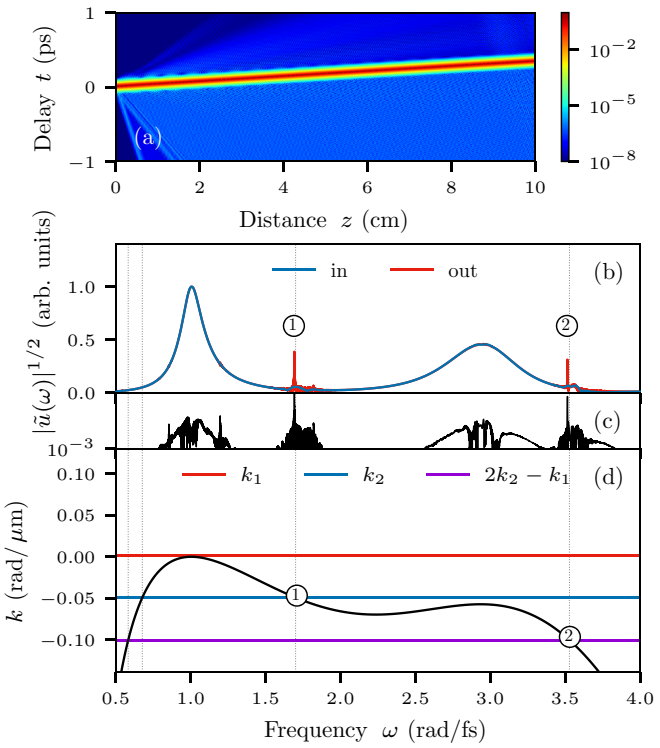

FIG. 1. Cherenkov radiation of an isolated two-color soliton molecule, produced by an initial condition with first-component carrier frequency $\omega_1 = 1.010$ rad/fs. (a) Time-domain view, (b) input and output spectra, (c) difference between both spectra on a logarithmic scale, and (d) diagram of the resonance conditions.

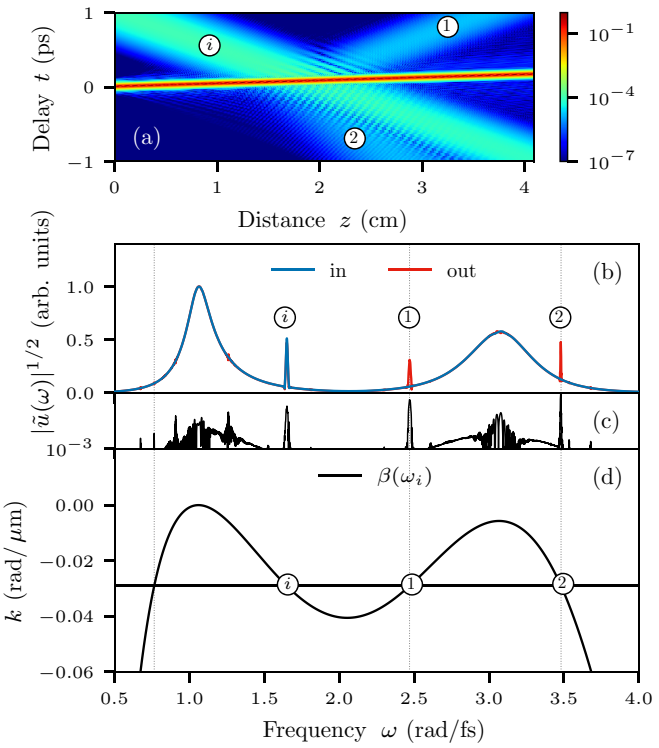

FIG. 2. Scattering of a weak DW with carrier frequency $\omega_{\text{inc}} = 1.650$ rad/fs on a two-color soliton with first-component carrier frequency $\omega_1 = 1.070$ rad/fs. (a) Time-domain view, (b) input and output spectra, (c) difference between both spectra on a logarithmic scale, and (d) diagram of the resonance conditions.

Below we set A_{inc} to 1% of the maximum amplitude of the isolated soliton and fix the width to $T_{\text{inc}} = 300$ fs. The initial pulse delay t_0 is chosen as ± 1000 fs from the soliton center, with the sign depending on the relative group velocity between the soliton and the DW and chosen so that both pulses engage in a collision. Upon propagation, the incident radiation interacts with the two-color soliton to produce scattered radiation. This process can evolve in several different ways depending on the frequencies of the soliton and the incident radiation. Below we consider three concrete examples. In each of them, the incident radiation is split between three different components.

The first configuration, shown in Fig. 2, is very close to the degenerate case where the wave numbers of the individual soliton components k_1 and k_2 coincide. Equation (13) then turns into Eq. (12). This case resembles the case of fundamental single-component solitons [36]; however, due to the shape of the dispersive curve $\beta(\omega)$, there is now more than one nontrivial solution to Eq. (12) and a single incident frequency yields up to four possible resonances. In practice, only some of them contribute to the scattered radiation. Those solutions are separately marked on a diagram in Fig. 2(d): ⓘ corresponds both to the incident and the partially transmitted radiation, ① is the reflected component, and ② is the additional transmitted component.

The second configuration, shown in Fig. 3, is a case with a significant difference between k_1 and k_2. Since Eq. (13) is no longer degenerate, the resonance diagram in Fig. 3(d) is more complex. However, as one can notice, in that case only the solution marked with ②, corresponding to the upper (i.e., "−, +") branch of Eq. (13), contributes to the scattered radiation. Component ①, corresponding to the scattered radiation, comes from resonance condition (12). The unmarked spectral line close to $\omega \approx 2.4$ rad/fs is the Cherenkov radiation of the soliton itself.

The third configuration, shown in Fig. 4, is in a sense symmetric to the previous case. Again, the difference between k_1 and k_2 is significant and Eq. (13) is far from being degenerate, but now the resonances from the lower (i.e., "+, −") branch of the resonance condition (13) play a significant role. This is achieved by choosing the incident frequency greater than the carrier frequency of the second soliton component and enhanced by using an asymmetric seed soliton with $T_1 = 30$ fs and $T_2 = 10$ fs. This creates a solitary wave with the amplitude of the second component almost equal to the amplitude of the first one.

Overall, in all of our experiments, only the scattered components corresponding to Eqs. (12) and (13) turn out to be significant, while the components predicted by Eqs. (14) and (15) do not seem to contribute to the resulting radiation. In other words, the terms proportional to $\tilde{\psi}^*_{\text{inc}}$ on the rhs of Eq. (11) can be safely neglected.

IV. NONLINEAR EFFECTS

When deriving resonance conditions (12)–(15), we assumed that the parameters of the solitons themselves stay

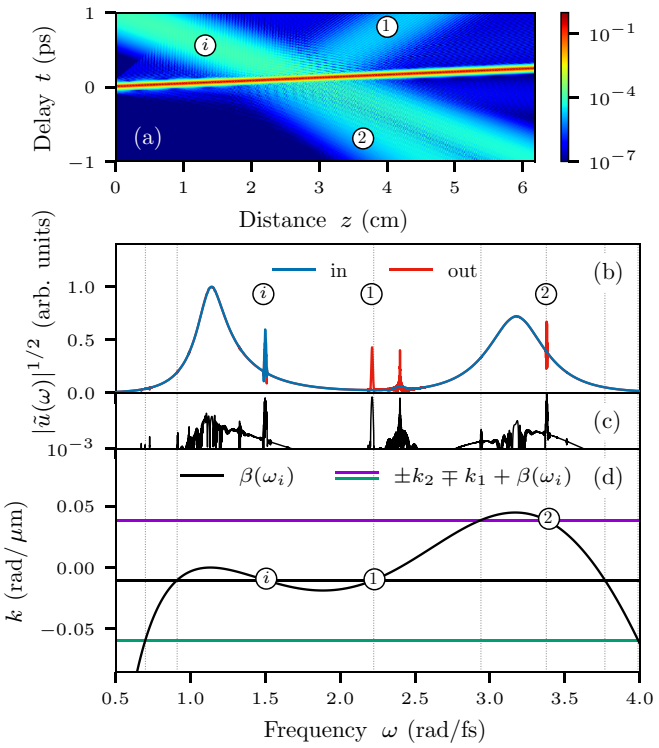

FIG. 3. Scattering of a weak DW with carrier frequency $\omega_{\text{inc}} = 1.500$ rad/fs on a two-color soliton with first-component carrier frequency $\omega_1 = 1.150$ rad/fs. (a) Time-domain view, (b) input and output spectra, (c) difference between both spectra on a logarithmic scale, and (d) diagram of the resonance conditions.

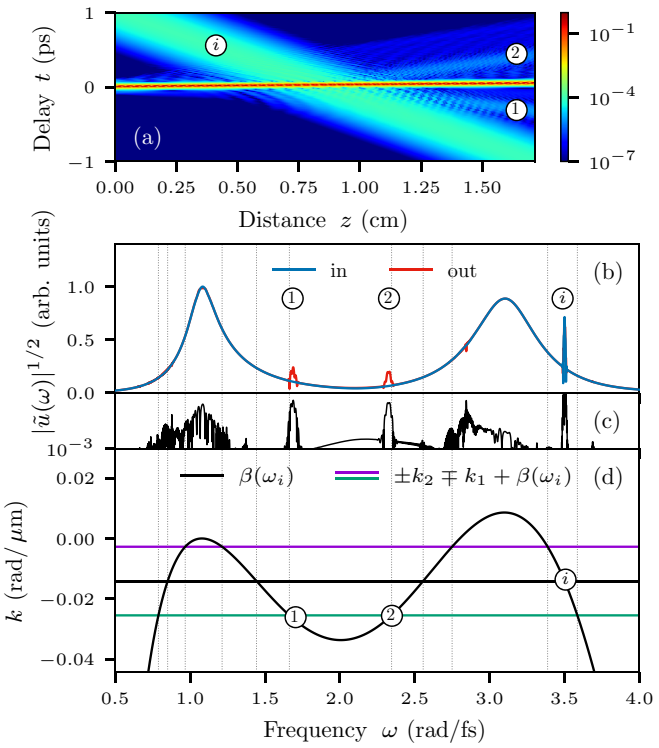

FIG. 4. Scattering of a weak DW with carrier frequency $\omega_{\text{inc}} = 3.500$ rad/fs on a two-color soliton with first-component carrier frequency $\omega_1 = 1.150$ rad/fs. (a) Time-domain view, (b) input and output spectra, (c) difference between both spectra on a logarithmic scale, and (d) diagram of the resonance conditions.

constant throughout the propagation and scattering processes. This can be considered a reasonable approximation when the amplitude of the incident wave is negligible compared to the amplitudes of the individual soliton components. However, in the general case of more intensive incident radiation, this assumption does not hold. In this section, we will briefly discuss two specific examples, where the process of scattering noticeably affects the parameters of the soliton. The general setup of the numerical experiments remains as in the preceding section, i.e., we consider scattering of a Gaussian pulse on an isolated two-color soliton, but this time we increase the amplitude of the DW to 5% of the soliton's maximum amplitude. This change might seem subtle, but it is sufficient to make the scattering dynamics much more involved.

In the first example, shown in Fig. 5, we consider scattering of a DW with incident frequency $\omega_i = 2.100$ rad/fs on a two-color soliton with $\omega_1 = 1.010$ rad/fs. From Fig. 5(a), we can immediately notice that interaction with the DW significantly decelerates the two-color soliton. This is connected to the change of the soliton's carrier frequency, as demonstrated in Fig. 5(b.2). This effect has been demonstrated before for the conventional solitons of a nonlinear Schrödinger equation [46,68]. What is remarkable about this interaction in the case of a two-color soliton is the fact that the soliton appears to be stable during this process. Granted, the frequency offset gained by the soliton during the scattering is not especially prominent [Fig. 5(b.2)], but at the same time, the amplitude

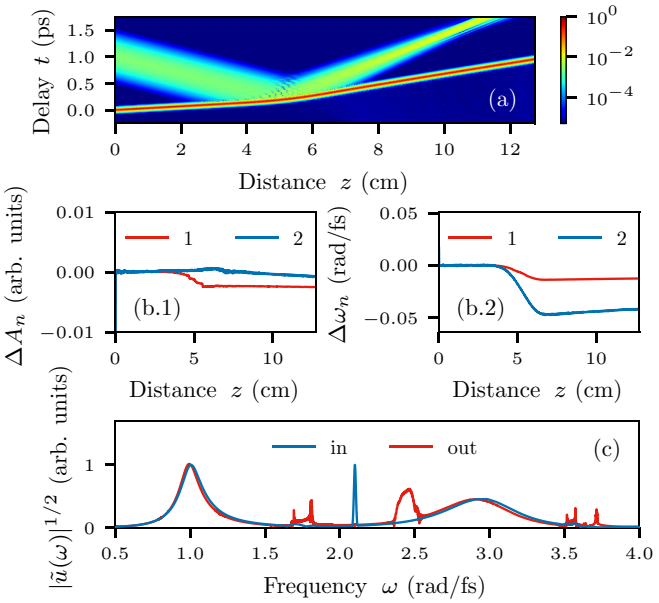

FIG. 5. Scattering of an intensive DW with carrier frequency $\omega_{\text{inc}} = 2.100$ rad/fs on a two-color soliton with first-component carrier frequency $\omega_1 = 1.010$ rad/fs. (a) Time-domain view. (b.1) Oscillation of the two-color soliton subpulse amplitudes. (b.2) Oscillation of the corresponding center frequencies. (c) Output spectrum.

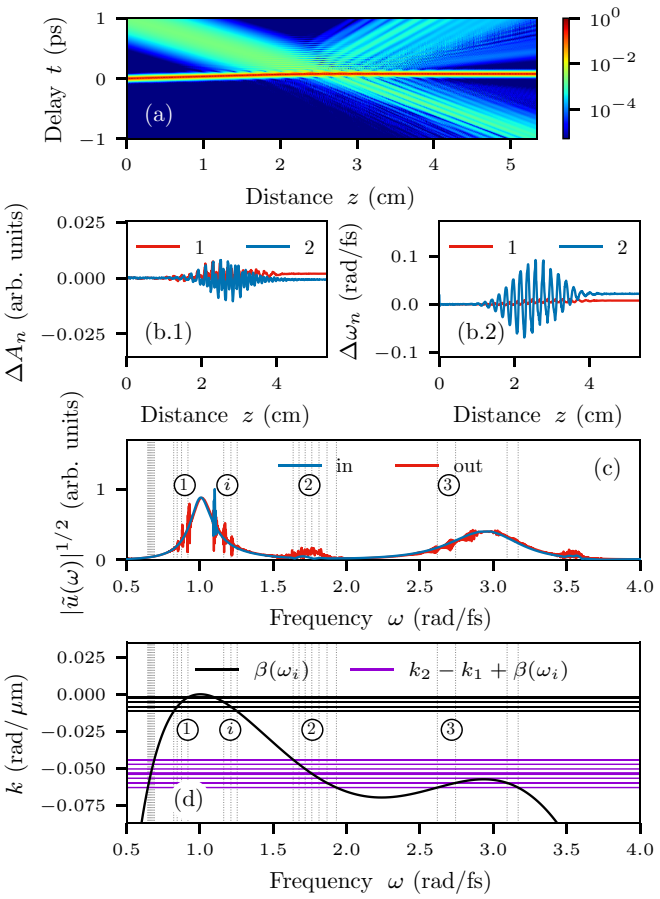

FIG. 6. Scattering of an intensive DW with carrier frequency $\omega_{\text{inc}} = 1.100$ rad/fs on a two-color soliton with first-component carrier frequency $\omega_1 = 1.010$ rad/fs. (a) Time-domain view. (b.1) Oscillation of the two-color soliton subpulse amplitudes. (b.2) Oscillation of the corresponding center frequencies. (c) Output spectrum. (d) Diagram of the resonance conditions.

difference in both of the frequency components stays under 1% [Fig. 5(b.1)], so almost no power loss occurs.

In the second example, shown in Fig. 6, we consider the scattering of a DW with the incident frequency $\omega_i = 1.100$ rad/fs on a two-color soliton with $\omega_1 = 1.010$ rad/fs. In the plots in Figs. 6(b.1) and 6(b.2), one can notice how the interaction with the DW generates oscillations in the soliton parameters; this is especially prominent in Fig. 6(b.2) that displays the absolute change of the soliton's central frequencies ω_1 and ω_2. From the latter plot, the period of those oscillations can be estimated as $Z_0 = 2$ mm. The interaction of freely oscillating nonlinear waves, including both the radiation and the scattering processes, is a well-studied problem [56–58,60,69] and the common trait in this setting, independent of the nature of the soliton oscillations, is that the dispersive radiation produced (generated or scattered) by the soliton is polychromatic, i.e., it consists of several isolated spectral components. This is indeed what we see in the output spectrum in Fig. 6(c).

To explain this behavior, let us return to Eqs. (6) and (11). In the oscillating case, the individual solitons U_1 and U_2 are no longer represented by a single spatial frequency $\propto e^{ik_1 z}$ and $\propto e^{ik_2 z}$, instead they correspond to a Fourier series,

$$U_n(z,t) = \sum_{N\in\mathbb{Z}} C_{nN}(t) \exp\left(ik_1 z + i\frac{2\pi N}{Z_0} z\right),$$

where Z_0 is the oscillation period. This leads to a split in the resonance conditions, and for the oscillating case equations (7), (8), (12), and (13) read

$$\beta(\omega) = k_n(\omega) + \frac{2\pi N}{Z_0}, \tag{7*}$$

$$\beta(\omega) = 2k_n(\omega) - k_m(\omega) + \frac{2\pi N}{Z_0}, \tag{8*}$$

$$\beta(\omega_{\text{sc}}) = \beta(\omega_{\text{inc}}) + \frac{2\pi N}{Z_0}, \tag{12*}$$

$$\beta(\omega_{\text{sc}}) = \pm k_1 \mp k_2 + \beta(\omega_{\text{inc}}) + \frac{2\pi N}{Z_0}, \tag{13*}$$

with $N \in \mathbb{Z}$ being the spatial harmonic number.

The resonance conditions for the scattering process in the last simulation are displayed in Fig. 6(d). In this process, only the last two equations, i.e., Eqs. (12*) and (13*), are relevant. The solid black lines correspond to Eq. (12) with harmonics $N = -3, \ldots, 0$. This harmonic split not only leads to the reflected part of the radiation ① becoming polychromatic, but also has the same effect on the incident component ⓘ. Resonance condition (13) is represented by the gray dashed lines for harmonics $N = -3, \ldots, +3$. It contributes to the scattered radiation twice: with a wide band ② that otherwise would degenerate into a sharp spectral line in a nonoscillating case, and with three wide spectral lines in the vicinity of ③ which is the contribution of the lower harmonics $N = -3, -2, -1$. One can notice that there are only two vertical lines corresponding to the numeric solution of Eq. (13) displayed around ③. This is merely due to a small numeric error in estimating the soliton wave number k_2 in the plotting procedure, which causes harmonic $N = -1$ to touch the dispersive rather than intersect it.

The specific oscillation mode we see in Fig. 6 appears to be heavily damped since launching the initial soliton with an additional frequency detuning does not lead to free frequency oscillations during the propagation. Such internal dynamics, reminiscent of molecular vibrations, were also reported previously [29,32], and the emission of DWs by the two-color soliton was found to explain the dampening of the oscillation mode [70]. Here, the incident radiation drives this oscillation and one could expect to observe a resonance behavior with respect to the frequency of the incident DW. And, indeed, as demonstrated by the parameter sweep in Fig. 7(a), by adjusting the incident frequency ω_i one can affect, to a certain degree, the amplitude of the frequency oscillations of the second component $\Delta\omega_2$. For this specific mode, where the frequency oscillations dominate, it is straightforward to get an estimate for the period Z_0 of the mode and the corresponding wave number K_0 in terms of a variational approach (see Appendix B). As shown in Fig. 7(b), superimposing the resulting resonance wave number K_0 on the dispersion curve allows one to graphically estimate the frequency of the incident DW that corresponds to the internal oscillation mode. The vertical dashed lines in Figs. 7(a) and 7(b) indicate this resonance fre-

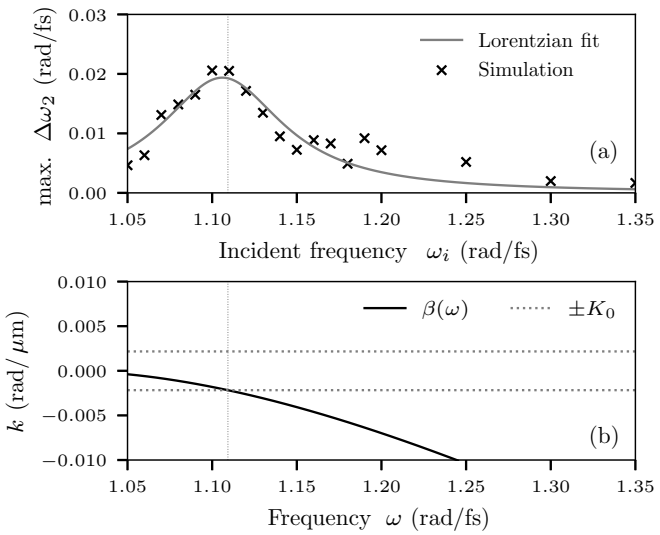

FIG. 7. Resonance behavior of the internal mode of the two-color soliton molecule during intensive scattering. (a) Oscillation of the center frequency of the second component of the two-color soliton as a function of the frequency of the incident DW. (b) Diagram of the resonance condition for the internal mode.

quency, confirming the excellent agreement of the numerical simulations and the approximate analytic estimate.

V. CONCLUSION

In this paper, we considered the resonant interaction of two-color soliton molecules with DWs. The resonance condition for Cherenkov radiation is derived and analyzed. The comparison with the results of numerical simulations shows that these conditions correctly predict the positions of the Cherenkov radiation. We also study the process of the collision of the two-color solitons with the incident DWs. The resonance conditions predict well all the generated frequencies observed in the numerical experiments. Some of the predicted resonances are not seen in the numerically calculated radiation spectra. This can be explained by the low efficiency of the corresponding scattering processes. The theory developed for a simpler case [37], involving a (single-pulse) soliton and a DW, shows that indeed for some parameters the generated radiation can be extremely weak. In the presented work, our focus was on deriving resonance conditions that allow one to estimate the location of resonant waves emitted by a two-color soliton in the presence of higher-order dispersion [Eq. (7)], as well as for further FWM processes internal to the two-color soliton molecule [Eq. (8)], and involving a two-color soliton molecule and an external DW [Eqs. (12)–(15)]. Although a theoretical framework for estimating the amplitudes of the resonant radiation could be established by extending the approach of Ref. [37] to the present case, this is out of the scope of the present study. Beyond deriving the above resonance conditions, we studied how the intensity of the incident dispersive waves affects the scattering. In particular, it is shown that the scattering can affect the soliton trajectory without affecting its integrity. Another important finding is that in the nonlinear case, the DWs can resonantly excite internal oscillations of the soliton. This results in polychromatic emission of DWs by oscillating two-color solitons. In this context, the resonant radiation due to Eqs. (7*) and (8*), caused by periodic amplitude and width variations of two-color soliton molecules, has been studied recently [71].

We believe that the results reported in this paper can possibly be used for optical supercontinuum generation. Another possible application is the spectroscopy of soliton molecules when some properties of the bound solitons can be extracted from the scattering data of the cw waves interacting with the solitons. Finally, we remark that similar effects can be anticipated to occur in molecules consisting of dark solitons. However, this constitutes an interesting problem of its own, which requires a separate consideration and will be addressed elsewhere.

ACKNOWLEDGMENTS

O.M., S.W., I.B., A.D., and U.M. acknowledge financial support from Deutsche Forschungsgemeinschaft (DFG) under Germany's Excellence Strategy within the Cluster of Excellence PhoenixD (Photonics, Optics, and Engineering–Innovation Across Disciplines) (EXC 2122, Project No. 390833453). S.B. acknowledges financial support from DFG under Germany's Excellence Strategy within the Cluster of Excellence QuantumFrontiers (EXC 2123, Project No. 390837967). A.Y. acknowledges financial support from Priority 2030 Academic Leadership Program and Goszadanie Grant No. 2019-1246. I.B. also acknowledges support from DFG (Project No. BA4156/4-2). U.M. also acknowledges support from DFG (Project No. MO 850-20/1).

APPENDIX A: DISPERSION PROFILE MODEL

We model dispersion coefficient $\beta(\omega)$ with the following rational expression:

$$\beta(\omega) = \frac{1}{c}\frac{\sum_{n=0}^{3} C_n \omega^{n+1}}{\sum_{m=0}^{3} D_m \omega^m}, \tag{A1}$$

where. $c = 0.29\,979\,245\,8$ μm/fs is the speed of light, and the coefficient sequences C and D are defined by

$$C = (9.654, -39.739\ \text{fs}, 16.885\ \text{fs}^2, -2.746\ \text{fs}^3), \tag{A2}$$

$$D = (1, -9.496\ \text{fs}, 4.221\ \text{fs}^2, -0.703\ \text{fs}^3). \tag{A3}$$

Here and throughout the paper, we assume fs as a unit of time and μm as a unit of distance. Figure 8 displays group velocity $v_g(\omega) = 1/\beta'(\omega)$ and second-order dispersion coefficient $\beta''(\omega)$ as functions of frequency. Frequencies ω_1 and ω_2 correspond to the central frequencies of the soliton's spectral components as chosen in the simulation corresponding to Fig. 1 of the paper.

APPENDIX B: SMALL INTERNAL OSCILLATIONS OF THE SOLITON

When analyzing the nonlinear scattering near an oscillatory mode, we used an expression for the oscillation frequency. In this section, we will derive this expression.

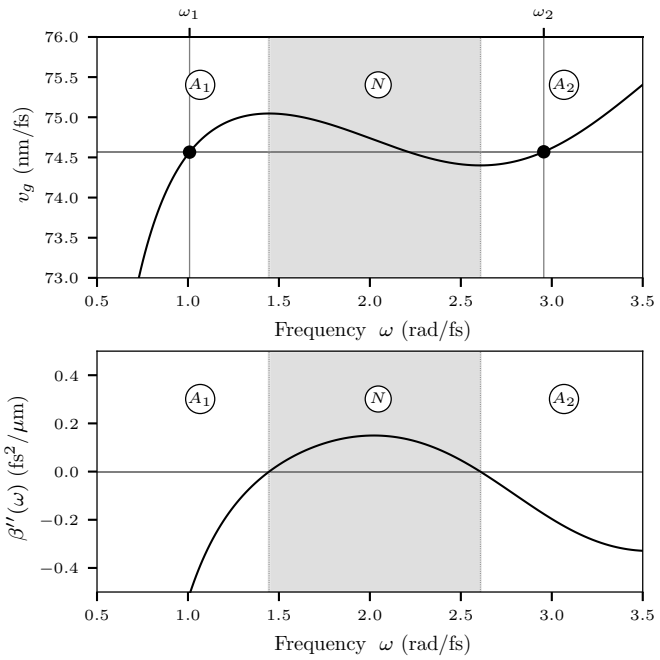

FIG. 8. (a) Group velocity v_g and (b) second-order dispersion coefficient $\beta''(\omega)$ in the model fiber. Labels $A_{1,2}$ and N mark the regions of anomalous and normal dispersion.

Let us return to Eq. (3) for coupled solitons. We can renormalize the equations by performing the following transformation:

$$U_n \to \gamma_n^{1/2} e^{i\beta_n z} U_n,$$

which will make the equations symmetric,

$$i\partial_z U_n - \tfrac{1}{2}\beta_n''\partial_t^2 U_n + \gamma_n^2 |U_n|^2 U_n + 2\gamma_n\gamma_m |U_m|^2 U_n = 0.$$

This in turn allows us to recognize the modified couple of equations as Euler-Lagrange equations for Lagrangian

$$\int_{-\infty}^{+\infty} \mathcal{L}(U_1, \partial_z U_1, \partial_t U_1, \ldots)\, dt,$$

where Lagrangian density $\mathcal{L}$ is defined as a sum of three components, $\mathcal{L} = \mathcal{L}_1 + \mathcal{L}_2 + \mathcal{L}_{\text{int}}$, with $\mathcal{L}_n$ being a single-soliton Lagrangian density,

$$\mathcal{L}_n = \frac{i}{2}(\partial_z U_n U_n^* - \partial_z U_n^* U_n) + \frac{1}{2}\beta_n''\, \partial_t U_n \partial_t U_n^* + \frac{1}{2}\gamma_n^2\, |U_n|^4, \tag{B1}$$

and $\mathcal{L}_{\text{int}}$ being the interaction term,

$$\mathcal{L}_{\text{int}} = 2\gamma_1\gamma_2 |U_1|^2 |U_2|^2. \tag{B2}$$

Let us assume that the soliton components U_n can be described by the following generic ansatz:

$$U_n(z,t) = A_n(z) S\left(\frac{t - t_n(z)}{\sigma_n(z)}\right) \exp[-i\Omega_n(z)t + i\phi_n(z)]. \tag{B3}$$

Here, A_n is the amplitude of the pulse, t_n is the central position, σ_n is the pulse width, Ω_n is the frequency detuning, ϕ_n is the phase, and $S(x)$ is a function that defines the envelope shape. At the moment, we will not specify the concrete form of $S(x)$, but will assume that it is an even function.

Before we continue, let us stress one important thing: this ansatz cannot express all the possible internal oscillations of the soliton. One obvious example, as was noted above, is the case of the pulse-width oscillation. In order to capture this dynamics, we need to add frequency chirp to the ansatz.

Substituting (B3) into (B1) and (B2) and integrating over t, we arrive at the expressions for the averaged Lagrangians,

$$L_n = I_1\, t_n \sigma_n A_n^2 \frac{d\Omega_n}{dz} + I_1\, \sigma_n A_n^2 \frac{d\phi_n}{dz} + I_2\, \frac{\beta_n''}{2}\frac{A_n^2}{\sigma_n} + I_1\, \frac{\beta_n''}{2}\sigma_n A_n^2 \Omega_n^2 + I_3\, \frac{\gamma_n^2}{2}\sigma_n A_n^4, \tag{B4}$$

$$L_{\text{int}} = 2\,\gamma_1\gamma_2\, A_1^2 A_2^2\, I_{\text{int}}(\sigma_1, \sigma_2, t_1, t_2), \tag{B5}$$

where the following integrals have been defined:

$$I_1 = \int_{-\infty}^{+\infty} S^2(x)\, dx, \quad I_2 = \int_{-\infty}^{+\infty} [S'(x)]^2\, dx,$$

$$I_3 = \int_{-\infty}^{+\infty} S^4(x)\, dx, \quad I_{\text{int}} = \int_{-\infty}^{+\infty} S^2\left(\frac{t - t_1}{\sigma_1}\right) S^2\left(\frac{t - t_2}{\sigma_2}\right) dt.$$

Due to the time invariance in the problem, I_{int} depends only on the difference between t_1 and t_2,

$$I_{\text{int}} = I_{\text{int}}(t_1 - t_2, \sigma_1, \sigma_2),$$

and it is an even function of that difference.

The averaged Lagrangian $L = L_1 + L_2 + L_{\text{int}}$ is now a function defined in terms of only the soliton parameters $\{A_n, \sigma_n, t_n, \Omega_n, \phi_n\}$. Therefore, the Euler-Lagrange equations for the new Lagrangian have to be defined in terms of variations over the soliton parameters,

$$\frac{\delta L}{\delta P_n} = \frac{\partial L}{\partial P_n} - \frac{d}{dz}\frac{\partial L}{\partial \dot{P}_n} = 0,$$

where P_n stands for either A_n, σ_n, t_n, Ω_n, or ϕ_n. The latter case—variation with respect to the phase ϕ_n—immediately yields the conservation of mass,

$$N_n = \sigma_n(z) A_n^2(z) = \text{const}. \tag{B6}$$

Variation with respect to the detuning Ω_n fixes the group velocity of individual solitons,

$$\frac{dt_n}{dz} = \beta_n''\Omega_n(z). \tag{B7}$$

Variation with respect to the soliton position t_n gives us an equation for the frequency,

$$\frac{d\Omega_n}{dz} = 2\frac{N_m\gamma_1\gamma_2}{I_1\sigma_1(z)\sigma_2(z)}\frac{\partial I_{\text{int}}}{\partial t_n}. \tag{B8}$$

The symmetry in the overlap integral I_{int} with respect to the soliton positions t_1 and t_2 leads to conservation of momentum,

$$N_1\Omega_1(z) + N_2\Omega_2(z) = \text{const}. \tag{B9}$$

Finally, the difference between the variations with respect to A_n and σ_n gives us

$$I_2\beta_n'' + \frac{I_3\gamma_n}{2}N_n\sigma_n(z) + 2N_m\gamma_1\gamma_2\frac{\sigma_n(z)}{\sigma_m(z)}\left(I_{\text{int}} + \sigma_n\frac{\partial I_{\text{int}}}{\sigma_n}\right) = 0. \tag{B10}$$

The very last equation—omitted here—is the evolution equation for the phase ϕ_n. The right-hand side of the equation is quite complicated, but since the phase does not occur anywhere in (B7), (B8), or (B10), it is not important for the remaining analysis.

Let us switch from the the individual soliton positions to the mean position and the relative delay instead,

$$t_0 = \tfrac{1}{2}(t_1 + t_2), \quad \Delta t = t_1 - t_2.$$

The equation for the relative delay Δt,

$$\frac{d\Delta t}{dz} = \beta_1'' \Omega_1(z) + \beta_2'' \Omega_2(z), \tag{B11}$$

and Eqs. (B8) and (B10) form a closed system, with equations for $d\Delta t/dz$, $d\Omega_n/dz$ acting as equations of motion and Eq. (B10) fixing the widths $\sigma_n(z)$ as functions of Δt. By differentiating (B11) one more time and using (B8), we get

$$\frac{d^2\Delta t}{dz^2} + 2\frac{\gamma_1\gamma_2(\beta_1''N_1 + \beta_2''N_2)}{I_1\sigma_1(\Delta t)\sigma_2(\Delta t)}\frac{\partial}{\partial \Delta t} I_{\rm int}(\Delta t, \sigma_1, \sigma_2) = 0.$$

To transform this into a harmonic oscillator equation, we need to linearize the second term around the equilibrium point $\Delta t = 0$. Since $I_{\rm int}$ is an even function, the derivative $\partial I_{\rm int}/\partial \Delta t$ is odd and it vanishes at $\Delta t = 0$. This means we can ignore Δt dependency in σ_1 and σ_2—only the term proportional to $\partial^2 I_{\rm int}/\partial \Delta t^2$ will survive. Thus we finally arrive at

$$\frac{d^2\Delta t}{dz^2} + K_0^2 \Delta t = 0,$$

where the resonance frequency K_0 is

$$K_0^2 = 2\frac{\gamma_1\gamma_2(\beta_1''N_1 + \beta_2''N_2)}{I_1\sigma_1(0)\sigma_2(0)} I_{\rm int}''[0; \sigma_1(0), \sigma_2(0)]. \tag{B12}$$

For a more concrete estimate, let us finally consider a Gaussian envelope, i.e., let us set $S(x) = \exp(-x^2)$. Such a choice of the envelope shape fixes the integrals $I_1 = \sqrt{\pi/2}$ and

$$I_{\rm int}(\Delta t, \sigma_1, \sigma_2) = \sqrt{\frac{\pi}{2}}\frac{\sigma_1\sigma_2}{\sqrt{(\sigma_1^2 + \sigma_2^2)}} \exp\left(\frac{-2\Delta t^2}{\sigma_1^2 + \sigma_2^2}\right),$$

which, finally, gives us the following expression for the resonance frequency:

$$K_0^2 = -\frac{8\,\gamma(\omega_1)\gamma(\omega_2)}{(\sigma_1^2 + \sigma_2^2)^{3/2}}\left[\beta''(\omega_1)\sigma_1 A_1^2 + \beta''(\omega_2)\sigma_2 A_2^2\right]. \tag{B13}$$

[1] J. M. Dudley, G. Genty, and S. Coen, Rev. Mod. Phys. **78**, 1135 (2006).
[2] D. V. Skryabin and A. V. Gorbach, Rev. Mod. Phys. **82**, 1287 (2010).
[3] J. M. Dudley and J. R. Taylor, *Supercontinuum Generation in Optical Fibers* (Cambridge University Press, Cambridge, 2010).
[4] L. F. Mollenauer and R. H. Stolen, Opt. Lett. **9**, 13 (1984).
[5] J. D. Kafka, T. Baer, and D. W. Hall, Opt. Lett. **14**, 1269 (1989).
[6] V. Matsas, T. Newson, D. Richardson, and D. Payne, Electron. Lett. **28**, 1391 (1992).
[7] S. K. Turitsyn, N. N. Rosanov, I. A. Yarutkina, A. E. Bednyakova, S. V. Fedorov, O. V. Shtyrina, and M. P. Fedoruk, Phys.-Usp. **59**, 642 (2016).
[8] M. Stratmann, T. Pagel, and F. Mitschke, Phys. Rev. Lett. **95**, 143902 (2005).
[9] A. Hause, H. Hartwig, M. Böhm, and F. Mitschke, Phys. Rev. A **78**, 063817 (2008).
[10] A. V. Buryak and N. N. Akhmediev, Phys. Rev. E **51**, 3572 (1995).
[11] B. A. Malomed, Phys. Rev. E **47**, 2874 (1993).
[12] A. Zavyalov, R. Iliew, O. Egorov, and F. Lederer, Phys. Rev. A **80**, 043829 (2009).
[13] Y. S. Kivshar and B. A. Malomed, Opt. Lett. **14**, 1365 (1989).
[14] F. K. Abdullaev, R. M. Abrarov, and S. A. Darmanyan, Opt. Lett. **14**, 131 (1989).
[15] N. N. Akhmediev, A. Ankiewicz, and J. M. Soto-Crespo, Phys. Rev. Lett. **79**, 4047 (1997).
[16] M. Haelterman, S. Trillo, and P. Ferro, Opt. Lett. **22**, 84 (1997).
[17] W. Weng, R. Bouchand, E. Lucas, E. Obrzud, T. Herr, and T. J. Kippenberg, Nat. Commun. **11**, 2402 (2020).
[18] D. Neshev, E. Ostrovskaya, Y. Kivshar, and W. Krolikowski, Opt. Lett. **28**, 710 (2003).
[19] V. V. Afanasjev and V. A. Vysloukh, J. Opt. Soc. Am. B **11**, 2385 (1994).
[20] E. N. Tsoy and F. K. Abdullaev, Phys. Rev. E **67**, 056610 (2003).
[21] Z. Chen, M. Acks, E. A. Ostrovskaya, and Y. S. Kivshar, Opt. Lett. **25**, 417 (2000).
[22] Y. V. Kartashov, L.-C. Crasovan, D. Mihalache, and L. Torner, Phys. Rev. Lett. **89**, 273902 (2002).
[23] G. Xu, A. Gelash, A. Chabchoub, V. Zakharov, and B. Kibler, Phys. Rev. Lett. **122**, 084101 (2019).
[24] X. Liu, X. Yao, and Y. Cui, Phys. Rev. Lett. **121**, 023905 (2018).
[25] K. Krupa, K. Nithyanandan, U. Andral, P. Tchofo-Dinda, and P. Grelu, Phys. Rev. Lett. **118**, 243901 (2017).
[26] U. Al Khawaja and A. Boudjemâa, Phys. Rev. E **86**, 036606 (2012).
[27] P. Grelu and N. Akhmediev, Nat. Photon. **6**, 84 (2012).
[28] B. Turmanov, B. Baizakov, B. Umarov, and F. Abdullaev, Phys. Lett. A **379**, 1828 (2015).
[29] O. Melchert, S. Willms, S. Bose, A. Yulin, B. Roth, F. Mitschke, U. Morgner, I. Babushkin, and A. Demircan, Phys. Rev. Lett. **123**, 243905 (2019).
[30] K. K. K. Tam, T. J. Alexander, A. Blanco-Redondo, and C. M. de Sterke, Phys. Rev. A **101**, 043822 (2020).
[31] O. Melchert and A. Demircan, Opt. Lett. **46**, 5603 (2021).
[32] O. Melchert, S. Willms, U. Morgner, I. Babushkin, and A. Demircan, Sci. Rep. **11**, 11190 (2021).
[33] J. P. Lourdesamy, A. F. J. Runge, T. J. Alexander, D. D. Hudson, A. Blanco-Redondo, and C. M. de Sterke, Nat. Phys. **18**, 59 (2022).

[34] G. Moille, Q. Li, S. Kim, D. Westly, and K. Srinivasan, Opt. Lett. **43**, 2772 (2018).
[35] O. Melchert, A. Yulin, and A. Demircan, Opt. Lett. **45**, 2764 (2020).
[36] A. V. Yulin, D. V. Skryabin, and P. S. J. Russell, Opt. Lett. **29**, 2411 (2004).
[37] D. V. Skryabin and A. V. Yulin, Phys. Rev. E **72**, 016619 (2005).
[38] A. Efimov, A. J. Taylor, F. G. Omenetto, A. V. Yulin, N. Y. Joly, F. Biancalana, D. V. Skryabin, J. C. Knight, and P. S. Russell, Opt. Express **12**, 6498 (2004).
[39] A. Efimov, A. V. Yulin, D. V. Skryabin, J. C. Knight, N. Joly, F. G. Omenetto, A. J. Taylor, and P. Russell, Phys. Rev. Lett. **95**, 213902 (2005).
[40] A. Efimov, A. J. Taylor, A. V. Yulin, D. V. Skryabin, and J. C. Knight, Opt. Lett. **31**, 1624 (2006).
[41] C. M. de Sterke, Opt. Lett. **17**, 914 (1992).
[42] A. V. Gorbach and D. V. Skryabin, Nat. Photon. **1**, 653 (2007).
[43] A. Demircan, S. Amiranashvili, C. Brée, and G. Steinmeyer, Phys. Rev. Lett. **110**, 233901 (2013).
[44] A. Demircan, S. Amiranashvili, C. Brée, C. Mahnke, F. Mitschke, and G. Steinmeyer, Sci. Rep. **2**, 850 (2012).
[45] T. G. Philbin, C. Kuklewicz, S. Robertson, S. Hill, F. Konig, and U. Leonhardt, Science **319**, 1367 (2008).
[46] A. Demircan, S. Amiranashvili, and G. Steinmeyer, Phys. Rev. Lett. **106**, 163901 (2011).
[47] A. V. Yulin, R. Driben, B. A. Malomed, and D. V. Skryabin, Opt. Express **21**, 14481 (2013).
[48] A. Demircan, S. Amiranashvili, C. Brée, U. Morgner, and G. Steinmeyer, Opt. Lett. **39**, 2735 (2014).
[49] S. F. Wang, A. Mussot, M. Conforti, X. L. Zeng, and A. Kudlinski, Opt. Lett. **40**, 3320 (2015).
[50] A. V. Yulin, Phys. Rev. A **98**, 023833 (2018).
[51] I. Oreshnikov, R. Driben, and A. V. Yulin, Opt. Lett. **40**, 4871 (2015).
[52] T. Marest, C. M. Arabí, M. Conforti, A. Mussot, C. Milián, D. V. Skryabin, and A. Kudlinski, Opt. Express **26**, 23480 (2018).
[53] Z. Deng, J. Liu, X. Huang, C. Zhao, and X. Wang, Opt. Express **26**, 16535 (2018).
[54] J. Rong, H. Yang, Y. Xiao, and Y. Chen, Phys. Rev. A **103**, 023505 (2021).
[55] Y. Kodama, M. Romagnoli, S. Wabnitz, and M. Midrio, Opt. Lett. **19**, 165 (1994).
[56] M. Conforti, S. Trillo, A. Mussot, and A. Kudlinski, Sci. Rep. **5**, 9433 (2015).
[57] R. Driben, A. V. Yulin, and A. Efimov, Opt. Express **23**, 19112 (2015).
[58] L. G. Wright, S. Wabnitz, D. N. Christodoulides, and F. W. Wise, Phys. Rev. Lett. **115**, 223902 (2015).
[59] K. Krupa, A. Tonello, A. Barthélémy, V. Couderc, B. M. Shalaby, A. Bendahmane, G. Millot, and S. Wabnitz, Phys. Rev. Lett. **116**, 183901 (2016).
[60] I. Oreshnikov, R. Driben, and A. Yulin, Phys. Rev. A **96**, 013809 (2017).
[61] N. Akhmediev and M. Karlsson, Phys. Rev. A **51**, 2602 (1995).
[62] V. V. Afanasjev, Y. S. Kivshar, and C. R. Menyuk, Opt. Lett. **21**, 1975 (1996).
[63] S. Amiranashvili and A. Demircan, Phys. Rev. A **82**, 013812 (2010).
[64] G. P. Agrawal, *Nonlinear Fiber Optics* (Academic Press, San Diego, 2013), p. 247.
[65] A. C. Hindmarsch, in *Scientific Computing*, edited by R. S. Stepleman, M. Carver, R. Peskin, W. F. Ames, and R. Vichnevetsky (North-Holland, Amsterdam, 1983), pp. 55–64.
[66] P. Virtanen, R. Gommers, T. E. Oliphant, M. Haberland, T. Reddy, D. Cournapeau, E. Burovski, P. Peterson, W. Weckesser, J. Bright *et al.*, Nat. Methods **17**, 261 (2020).
[67] https://github.com/ioreshnikov/two-color-solitons.
[68] L. Tartara, J. Opt. Soc. Am. B **32**, 395 (2015).
[69] I. Oreshnikov, R. Driben, and A. Yulin, Opt. Lett. **40**, 5554 (2015).
[70] S. Willms, O. Melchert, S. Bose, A. Yulin, I. Oreshnikov, U. Morgner, I. Babushkin, and A. Demircan, Phys. Rev. A **105**, 053525 (2022).
[71] O. Melchert, S. Willms, I. Oreshnikov, A. Yulin, U. Morgner, I. Babushkin, and A. Demircan, arXiv:2208.13829v1.